

Large-eddy simulations of a reactive jet in supersonic cross-flow based on a hybrid model of turbulent combustion

Anthony Techer*, Radouan Boukharfane^{*,**}, Guillaume Lehnasch*, Arnaud Mura*

* Institut PPRIME UPR 3346 CNRS - ENSMA - Université de Poitiers, 86961 Futuroscope, France

** DAEP, ISAE-SUPAERO, 10 Avenue Edouard Belin, Toulouse, 31055, France

1. Introduction

Since it provides efficient mixing and combustion stabilization in high-speed regimes, the jet in supersonic cross-flow (JISCF) is considered as a geometry of reference for Scramjet applications. However, despite significant progresses made in the experimental analysis of this configuration [1], the understanding of the corresponding turbulent reactive flows still remains incomplete from a quantitative viewpoint. The detailed experimental characterization of such a complex three-dimensional flow topology indeed poses severe difficulties for diagnostics and it exhibits quite a significant sensitivity to the variations of flow parameters, e.g., nozzle pressure ratio (NPR) and momentum flux ratio. For instance, the latter is known to influence jet penetration and trajectory [2, 3] as well as the global structure of the stabilization zone [1]. As a consequence, high-fidelity numerical simulations offer an interesting and complementary alternative to experiments so as to improve our understanding of such complicated flowfields. In particular, today's computational resources make possible the achievement of highly resolved large-eddy simulations (LES), which has become a popular strategy to perform the analysis of such supersonic turbulent reactive flows [4, 5]. In this study, highly resolved LES of sonic transverse hydrogen jets in a vitiated air cross-flow at Mach 2 are reported. A new hybrid model of turbulent combustion, hereafter denoted by HTC, is presented. The results obtained with this subgrid-scale (SGS) closure are compared to those issued from the consideration of the standard perfectly stirred reactor (PSR), which is also often referred to as quasi laminar chemistry or quasi-laminar chemistry model. The latter indeed ignores the possible influence of residual SGS fluctuations of composition, the description of which has been central to a recent non-reactive flow study of the same JISCF geometry [6]. Compared to the PSR model, the present HTC modelling proposal aims at taking into account their possible influence, while accommodating the constraint that the SGS combustion model should recover the DNS limit as the filter size tends to zero. It will be shown that, whatever the closure retained to represent the influence of SGS fluctuations on the filtered chemical rate, the proposed framework may be thought as a general modelling procedure to enforce this specific rule. Some preliminary results are considered to test the relevance of this proposal. They correspond to qualitative comparisons since no experimental measurements are available for the simplified computational geometry that has been considered. The present objective is only to measure the possible influence of taking (or not) into account the SGS fluctuations of composition on the general topology of the compressible reactive flowfield.

2. Numerical setup and simulation parameters

The computational solver used to conduct this study is the in-house massively-parallel solver CREAMS. Its characteristics have been previously detailed in references [7, 8] and only its salient features are briefly summarized. The treatment of the inviscid component of the Navier-Stokes transport equations relies on the seventh-order accurate weighted essentially non-oscillatory (WENO7) reconstruction of the characteristic fluxes [9]. In practice, the solver uses a high-order accuracy finite difference scheme, and the application of the non-linear weighting procedure of the WENO7 scheme is conditioned to a shock sensor that involves the local values of the normalized spatial variations of both pressure and density. Finally, the viscous and molecular diffusion flux functions are determined thanks to an eighth-order centered finite difference scheme. The temporal integration is performed with an explicit third-order total-variation-diminishing (TVD) Runge-Kutta scheme [10]. For the purpose of the present study, the spatially filtered reactive compressible Navier-Stokes equations are solved and the detail of the retained formulation can be found elsewhere [6]. Throughout the manuscript, the spatially filtered value and density-weighted spatially filtered value of any quantity φ are denoted by $\bar{\varphi}$ and $\tilde{\varphi}$, respectively, while $\check{\varphi}$ is a resolved contribution, e.g., $\check{\omega}_\alpha = \check{\omega}_\alpha(\bar{p}, \tilde{T}, \tilde{Y})$ is the resolved production rate of species α .

The dimensions of the computational domain are $190.0D \times 8.85D \times 20.0D$, where D denotes the diameter of the jet exit, which is located on the bottom wall and centered along the spanwise z -direction. It is discretized with a Cartesian grid featuring $N_x \times N_y \times N_z = 2253 \times 196 \times 193$; that is, approximately 85,200,000 computational points. The corresponding grid is refined in the boundary layer and gradually stretched from the bottom wall to the upper boundary. The near-wall computational resolution has been examined in further detail by scrutinizing the values of Δx^+ , Δy^+ , and Δz^+ , which denote the dimensions of the computational cells present at the wall location expressed in wall units¹, i.e., $\Delta x^+ = \Delta x/l_w$, $\Delta y^+ = \Delta y/l_w$, and $\Delta z^+ = \Delta z/l_w$. In the near-wall region and in the vicinity of the jet exit, the average values of Δy^+ lie within [0.4,1.2], while the average values of Δx^+ and Δz^+ remain bounded within the ranges [13.0,30.0] and [10.0,40.0], respectively. The boundary conditions are imposed as follows: the fuel mass flow rate is set to $1.85 \text{ g} \cdot \text{s}^{-1}$, the total temperature $T_{t,jet}$ is approximately equal to 300 K. This corresponds to a static temperature $T_{jet} = 248.4 \text{ K}$, a bulk velocity $u_{jet} = 1204 \text{ m} \cdot \text{s}^{-1}$, and a static pressure $p_{jet} = 502918 \text{ Pa}$. The fuel density is $\rho_{jet} = 0.491 \text{ kg} \cdot \text{m}^{-3}$. The velocity profile is imposed with an error function and accounts for the presence of boundary layers at the injection condition. The supersonic flow of vitiated air consists of three chemical species (O_2 , N_2 , H_2O) with mass fractions (0.2527, 0.1631, 0.5842). It is characterized by a Mach number value $M_\infty = 2.0$, a total pressure $p_{t,\infty} = 0.409 \text{ MPa}$ and a total temperature $T_{t,\infty} = 1695 \text{ K}$, which correspond to a velocity of approximately $1313 \text{ m} \cdot \text{s}^{-1}$ while the density is about $0.161 \text{ kg} \cdot \text{m}^{-3}$. For the present flow conditions, the momentum flux ratio between the hydrogen jet and the transverse flow of vitiated air is approximately $J = 2.56$ and the global equivalence ratio is $\Phi = 0.4$. These conditions are representative of those considered in the dual mode ramjet investigations conducted on the LAPCAT-II setup [11].

3. Presentation of the hybrid turbulent combustion (HTC) model

Some details about the derivation of the HTC model are now presented. The segregation-rate S_ξ of a passive scalar (i.e., the mixture fraction ξ) is first introduced to estimate the departures from the perfectly-stirred reactor (PSR) limit. It can be determined from the filtered mixture fraction $\tilde{\xi}$ and SGS variance $\tilde{V}_\xi = \tilde{\xi}^2 - (\tilde{\xi})^2$.

¹We recall that the wall unit l_w is given by $l_w = \mu_w / \sqrt{\rho_w \tau_w}$, with τ_w the mean shear stress at the walls.

Its value, which is evaluated from $S_\xi = \tilde{V}_\xi / (\tilde{\xi}(1 - \tilde{\xi}))$, remains bounded between zero and unity. Following a strategy similar to the one previously presented in reference [12], it will be presently used as a weighting coefficient between two contributions so as to express the filtered chemical production rate of any species α

$$\tilde{\omega}_\alpha(p, T, \mathbf{Y}) = (1 - S_\xi) \cdot \dot{\omega}_\alpha(\bar{p}, \tilde{T}, \tilde{\mathbf{Y}}) + S_\xi \cdot \tilde{\omega}_\alpha^{\text{SGS}} \quad (1)$$

where the first term of the right hand side (RHS) corresponds to the resolved contribution, while the second one represents the SGS contribution. Except for the weighting coefficient, such a representation displays some similarities with an asymptotic development in function of the Damköhler number Da , such as the one early proposed by Borghi [13], the first contribution can be associated to the lowest-order term in Da , while the second gathers the effects of all the other higher-order terms. It must be emphasized that such a decomposition implicitly assumes that the influence of SGS composition fluctuations can be followed through the use of the mixture fraction only. Finally, it must be emphasized that, as the filter size Δ tends to ϵ (with ϵ any arbitrary small number), the SGS fluctuations of composition tends to zero. Accordingly, in these conditions, we have $S_\xi = 0$ in Eq. 1 in such manner that the filtered chemical production rate of any chemical species α becomes strictly equal to its resolved counterpart: the DNS limit is recovered.

Contribution of the resolved part. It is the first term present in the RHS of Eq.1. It is estimated directly from the filtered values of pressure, density, temperature, and species mass fractions by using a chemical scheme, which includes a satisfactory description of the self-ignition chemistry [14]. It should be emphasized that this contribution assumes that the reactive medium is fully premixed and corresponds to a PSR estimation.

Contribution of the sub-grid scale part. In contrast with the resolved contribution, the second term of the RHS of Eq. 1 requires an explicit closure. The corresponding closure should accommodate with various regimes of turbulence-chemistry interactions (TCI) and combustion modes including premixed, partially premixed, and possible non-premixed combustion conditions in the direct vicinity of the fuel nozzle jet exit. It is clear that the elaboration of such a general closure still remains an open issue. Following the introduction of the Takeno's index [15], some attempts were made in this direction using a premixedness index² with the SGS chemical production rate decomposed into two distinct contributions: $\tilde{\omega}_\alpha^{\text{SGS}} = (1 - \check{\zeta}_P) \tilde{\omega}_\alpha^{\text{SGS,NP}} + \check{\zeta}_P \tilde{\omega}_\alpha^{\text{SGS,P}}$ but it must be acknowledged that a general definition of $\check{\zeta}_P$ is still missing. For the sake of simplicity, it is therefore chosen to consider only the non-premixed combustion contribution at the subgrid-scale level and it is thus assumed $\tilde{\omega}_\alpha^{\text{SGS}} = \tilde{\omega}_\alpha^{\text{SGS,NP}}$. This is supported by the fact that, in the present JISCF geometry, according to Eq. 1, the SGS contribution is expected to be the largest in the vicinity of the separate (i.e., non-premixed) injection of fuel in the vitiated airstream, where the segregation-rate S_ξ is large. Among the large variety of existing turbulent non-premixed combustion models, we retain a closure that approximates the Lagrangian trajectory in the composition space. The main reason for this choice is that the corresponding closure has recently been implemented in the CREAMS solver. The Modèle Intermittent Lagrangien (MIL) was early proposed to address finite-rate chemistry effects [16]. It has been previously established to be robust and quite easy to implement, and it features low computational costs in such a manner that it has been applied to a large variety of situations including non-premixed combustion [16, 17], two-phase flow combustion [18, 19], and combustion in non-premixed high-speed flows [20]. Thus, the corresponding model provides a closure for the SGS contribution $\tilde{\omega}_\alpha^{\text{SGS,NP}} = \tilde{\omega}_\alpha^{\text{MIL}}$, the details of which can be found elsewhere. In the next sections, we will report the results of computations performed using either the PSR approximation (i.e., $\tilde{\omega}_\alpha(p, T, \mathbf{Y}) = \dot{\omega}_\alpha(\bar{p}, \tilde{T}, \tilde{\mathbf{Y}})$) or the model deduced from Eq. 1, that is $\tilde{\omega}_\alpha = (1 - S_\xi) \dot{\omega}_\alpha(\bar{p}, \tilde{T}, \tilde{\mathbf{Y}}) + S_\xi \tilde{\omega}_\alpha^{\text{MIL}}$.

²The value of this index is evaluated at the resolved scale.

4. Results and discussion

Figure 1 reports a typical snapshot of the flowfield structure obtained at $t^* = t \cdot u_\infty / D = 170.0$ using either the PSR model or the HTC model. The topologies of both flowfields clearly display visible differences. In the direct vicinity of the injection (i.e., downstream of the barrel shock), the chemical reaction takes place close to the wall but the extension of the region where it proceeds remains limited in both height and width. This is in contrast with the results obtained using the PSR model since, in this case, no chemical reaction occurs and no radicals or combustion products are formed at this location. In this region, the filtered composition indeed remains outside the ignition limits while, within the HTC framework, the probability to lie within these limits is not zero. It is also noteworthy that, with the HTC model, the obtained results depict a weakly reactive zone in the wake of the injection: the production of the OH radicals is limited but non-zero, whereas the PSR model does not exhibit any production of OH radicals at the same location. In the far field, at first glance, the flame structure seems to be similar for both simulations. Finally, compared to the PSR model, the HTC model displays a smaller amount of production of OH radicals at the foot of the bow shock that establishes upstream of the injector.

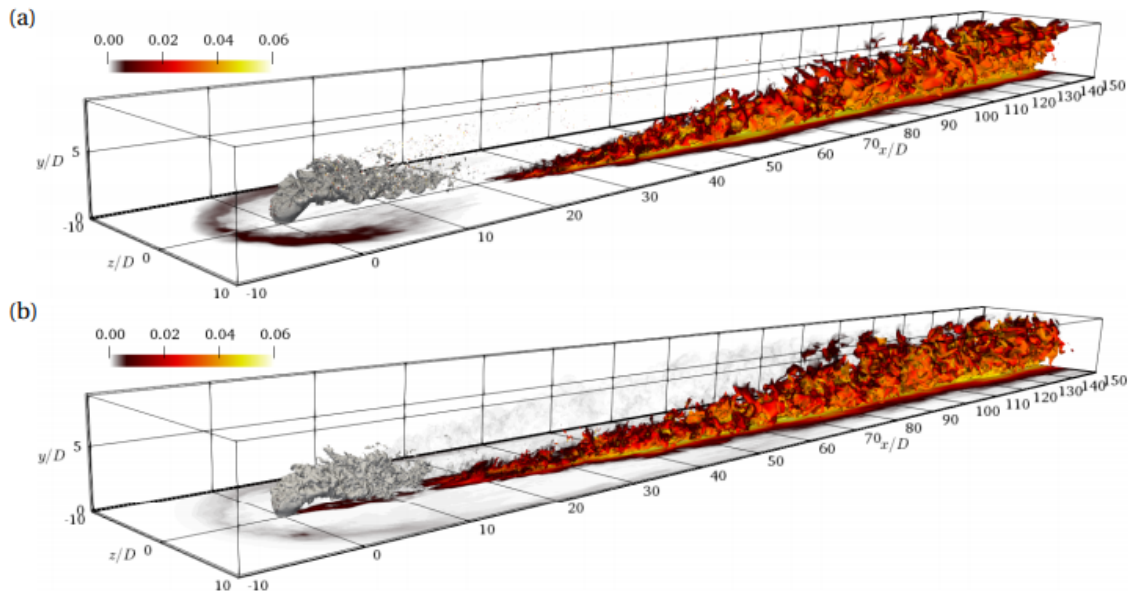


Figure 1: Comparison at $t^* = 170.0$ of the instantaneous flame structure obtained with (a) the PSR model and (b) the HTC model. Iso-surface of the stoichiometric mixture fraction $\tilde{\xi}_{st}$ colored by the molar fraction X_{OH} and parietal field of the same quantity. The grey iso-surface corresponds to $\tilde{\xi} = 0.5$.

Figure 2 compares the fields of normalized filtered temperature \tilde{T}/T_∞ , filtered heat-release rate $\tilde{\omega}_T$, reactivity λ [14], and mass fractions of OH and HO₂ in the (x, y) mid-plane ($z = 0$). This figure confirms that, with the HTC model, the stabilization of the reactive zone takes place rather closer to the injection port, downstream of it, and in the near wall. The HTC model also predicts that the width of the development of the reactive zone is larger. Thus, although the filtered heat release evaluated with one or another of the two methods are of the same order of magnitude, the consideration of the SGS contribution is sufficient (i) to favor an early stabilization of the reactive zone and (ii) to induce a larger expansion of the burned gases further downstream of the hydrogen injection. With the HTC model, the high reactivity λ region seems to be less extended (along the y -direction) in

the far field but it is also noteworthy that it is more important at locations just upstream of the injection. Therefore, self-ignition may occur in this region. However, the corresponding region is also associated to rather large values of the segregation-rate S_ξ , which may restrict its occurrence since the values of $(1 - S_\xi)\omega_\alpha^{\text{PSR}}$ remains limited. It is also noteworthy that the SGS contribution, as evaluated from the MIL model, remains negligible at this location. In this respect, it should be emphasized that models based on the mixture fraction PDF, such as the MIL model or any steady laminar non-premixed flamelet (SLF) model, since they do not consider chemical reactions in either the oxidizer or the fuel inlet streams, are unable to recover certain finite rate chemistry effects, such as those associated to dissociation taking place downstream of a shock-wave in the oxidizer stream.

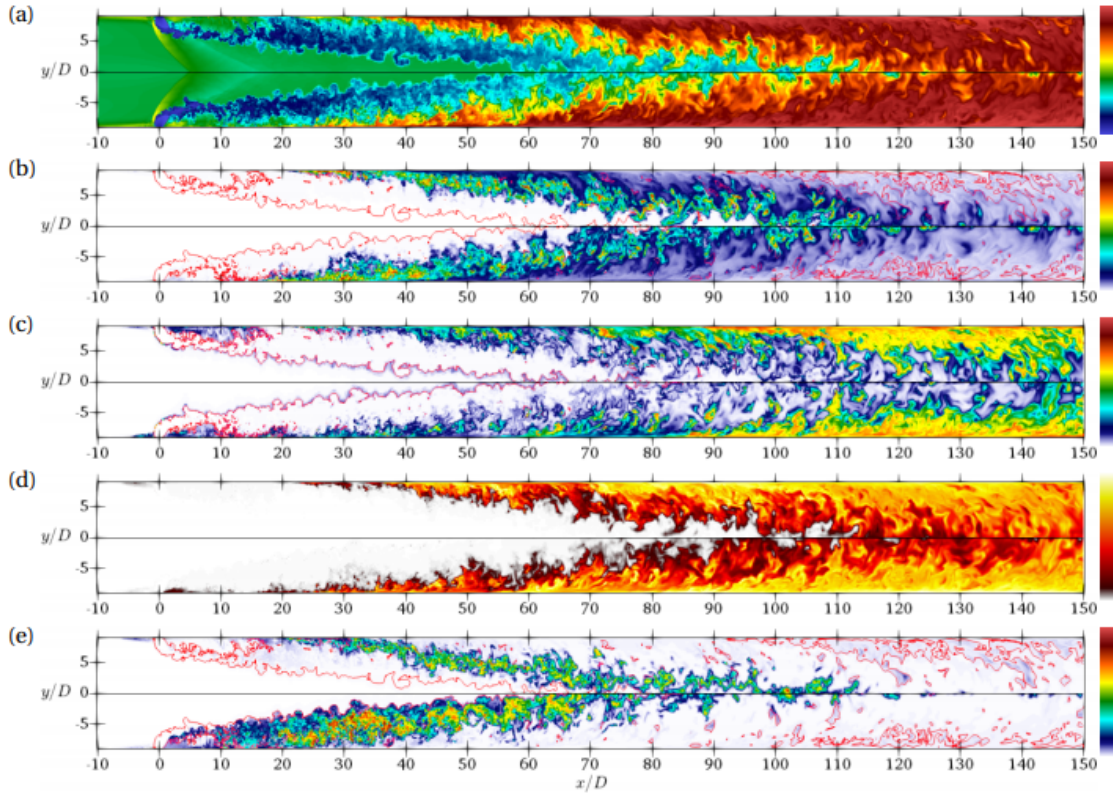


Figure 2: Comparison at $t^* = 170.0$ of the fields of (a) the normalized filtered temperature $\tilde{T}/T_\infty[0.04, 2.5]$, (b) heat release rate $\tilde{\omega}_T[0, 1.6 \times 10^{11}]$ W/kg, (c) reactivity $\lambda[0, 10^6]$ s, (d) $Y_{\text{OH}}[0, 0.04]$, and (e) $10^3 \times Y_{\text{HO}_2}[0, 0.953]$ obtained with the PSR (top) or HTC model (bottom). The red iso-line corresponds to $\xi_{st} = 0.03$.

5. Conclusions and future works

A new LES closure is introduced to describe possible departures from the PSR limit in reactive high-speed flows. It is applied to the numerical simulation of a reactive hydrogen jet in supersonic cross-flow (JISCF) in conditions relevant to scramjet engine propulsion. The main features of the resulting computational flowfield are analyzed and compared to those obtained with the more standard and widely-used PSR model, which is also often referred to as quasi laminar chemistry or quasi-laminar approach. As expected, the most striking differences are obtained in the near-field of the hydrogen jet injection, where the impact of residual SGS fluctuations of composition may indeed be non-negligible. A more quantitative inspection of the present set of data

is currently in progress, especially, some complementary statistical analyses would be welcome to satisfy the reader's (and the authors') curiosity.

References

- [1] M. Gamba and M. G. Mungal, Ignition, flame structure and near-wall burning in transverse hydrogen jets in supersonic crossflow, *J. Fluid Mech.*, vol. 780, p. 226-273, 2015.
- [2] A. Ben-Yakar, M. G. Mungal, and R. K. Hanson, Time evolution and mixing characteristics of hydrogen and ethylene transverse jets in supersonic crossflows, *Phys. Fluids*, vol. 18, no. 2, p. 026101, 2006.
- [3] X. Chai, P. S. Iyer, and K. Mahesh, Numerical study of high speed jets in crossflow, *J. Fluid Mech.*, vol. 785, p. 152-188, 2015.
- [4] Y. Moule, V. Sabelnikov, and A. Mura, Highly resolved numerical simulation of combustion in supersonic hydrogen-air coflowing jets, *Combust. Flame*, vol. 161, no. 10, pp. 2647-2668, 2014.
- [5] R. Buttay, G. Lehnasch, and A. Mura, Highly resolved numerical simulation of combustion downstream of a rocket engine igniter, *Shock Waves*, vol. 27, pp. 655-674, 2017.
- [6] A. Techer, Y. Moule, G. Lehnasch, and A. Mura, Mixing of a fuel in a supersonic crossflow: Estimation of subgrid-scale scalar fluctuations, *AIAA J.*, vol. 56, no. 2, pp. 465-481, 2018.
- [7] P.J. Martínez-Ferrer, R. Buttay, G. Lehnasch, and A. Mura, A detailed verification procedure for compressible reactive multicomponent Navier-Stokes solvers, *Comput. Fluids*, vol. 89, pp. 88-110, 2014.
- [8] R. Boukharfane, F. Ribeiro, Z. Bouali, and A. Mura, A ghost-point-forcing / direct-forcing immersed boundary method for compressible flow simulations, *Comput. Fluids*, vol. 162, pp. 91-112, 2018.
- [9] D. Balsara and C. Shu, Monotonicity preserving weighted essentially non-oscillatory schemes with increasingly high-order of accuracy, *J. Comput. Phys.*, vol. 106, pp. 405-452, 2000.
- [10] S. Gottlieb and C. W. Shu, Total variation diminishing Runge-Kutta schemes, *Mathematics of computation of the American Mathematical Society*, vol. 67, no. 221, pp. 73-85, 1998.
- [11] A. Vincent-Randonnier, Y. Moule, and M. Ferrier, Combustion of hydrogen in hot air flows within the LAPCAT-II Dual Mode Ramjet combustor at Onera-LAERTE facility. *AIAA Paper 2014-2932*.
- [12] A. Mura, V. Robin, and M. Champion, Modeling of scalar dissipation in partially premixed turbulent flames, *Combust. Flame*, vol. 149, no. 1-2, pp. 217-224, 2007.
- [13] R. Borghi, Computational studies of turbulent flows with chemical reactions, in: *Turbulent Mixing in Non Reactive and Reactive Flows*, S. N. B. Murthy (Ed.), Plenum Press (New York), 1975, pp. 163-188.
- [14] P. Boivin, C. Jiménez, A. L. Sánchez, and F. A. Williams, An explicit reduced mechanism for H₂-air combustion, *Proc. Combust. Inst.*, vol. 33, no. 1, pp. 517-523, 2011.
- [15] H. Yamashita, M. Shimada, and T. Takeno, A numerical study on flame stability at the transition point of jet diffusion flames, in *Symposium (Int.) on Combustion*, vol. 26, no. 1, 1996, pp. 27-34.
- [16] M. Obounou, M. Gonzalez, and R. Borghi, A Lagrangian model for predicting turbulent diffusion flames with chemical kinetic effects, *Symposium (Int.) on Combustion*, vol. 25, no. 1, 1994, pp. 1107-1113.
- [17] A. Mura and F.-X. Demoulin, Lagrangian intermittent modelling of turbulent lifted flames, *Combust. Theory Modell.*, vol. 11, no. 2, pp. 227-257, 2007.
- [18] F.-X. Demoulin and R. Borghi, Modeling of turbulent spray combustion with application to diesel like experiment, *Combust. Flame*, vol. 129, no. 3, pp. 281-293, 2002.

- [19] L. Gomet, V. Robin, and A. Mura, Lagrangian modelling of turbulent spray combustion under liquid rocket engine conditions, *Acta Astronautica*, vol. 94, no. 1, pp. 184-197, 2014.
- [20] J.-F. Izard, G. Lehnasch, and A. Mura, A Lagrangian model of combustion in high-speed flows: Application to scramjet conditions, *Combust. Sci. Technol.*, vol. 181, no. 11, pp. 1372-1396, 2009.